ISSN 1070-3632, Russian Journal of General Chemistry, 2015, Vol. 85, No. 1, pp. 135–143. © Pleiades Publishing, Ltd., 2015.
Original Russian Text © P.A. Stabnikov, I.V. Korol'kov, N.V. Pervukhina, O.V. Antonova, P.E. Plyusnin, S.A. Prokhorova, S.V. Larionov, 2015, published in Zhurnal Obshchei Khimii, 2015, Vol. 85, No. 1, pp. 144–153.

Synthesis, Structure, Thermal, and Photoluminescent Properties of Europium(III) and Terbium(III) Dipivaloylmethanates with N-Heterocyclic Compounds

P. A. Stabnikov[a], I. V. Korol'kov[a,b], N. V. Pervukhina[a], O. V. Antonova[a], P. E. Plyusnin[a,b], S. A. Prokhorova[a], and S. V. Larionov[a,b]

[a] *Nikovaev Institute of Inorganic Chemistry, Siberian Branch, Russian Academy of Sciences, pr. Akademika Lavrent'eva 3, Novosibirsk, 630090 Russia*
e-mail: stabnik@niic.nsc.ru

[b] *Novosibirsk State University, Novosibirsk, Russia*

Received July 17, 2014

Abstract—Mixed-ligand complexes of Eu(III) and Tb(III) dipivaloylmethanates with N-heterocyclic ligands (3,5-dimethylpyrazole, imidazole, 4-aminopyridine, 2,2'-bipyridine, and 1,10-phenanthroline) were synthesized. X-ray diffraction analysis was used to determine the structure of the dimer $Eu_2(dpm)_6$ and mononuclear complexes $Ln(dmpz)(dpm)_3$ (Ln = Eu, Tb) and $Tb(apy)(dpm)_3$. Photoluminescence of the complexes and their films obtained by chemical vapor deposition was studied.

Keywords: lanthanide β-diketonates, N-heterocyclic ligands, structure, luminescence, volatility

DOI: 10.1134/S1070363215010235

Lanthanide (Ln) complexes with β-diketones are used as a material in the manufacturing of electro- and photoluminescent devices [1–3]. Owing to their volatility, these compounds can serve as precursors for coating manufactured by the MOCVD technology [4]. An efficient way to control the luminescence intensity of Ln complexes is to synthesize mixed-ligand complexes containing, along with β-diketonate anions, N-heterocycles which can act as fluorophores. One of the β-diketonate ligands is dipivaloylmethanate (dpm). Metal chelates with this ligand are thermally stable and volatile [5, 6].

At present mixed-ligand complexes of Ln dipialoylmethanate with N-heterocyclic ligands have scarcely been studied. Synthesis and structural characterization have been reported for $Eu(py)_2(dpm)_3$ [7], $Lu(mepy)(dpm)_3$ (mepy = 3-methylpyridine) [8], $Tb(me_2apy)(dpm)_3$ and $Sm(me_2apy)(dpm)_3$ (me_2apy = 4-dimethylaminopyridine) [9], $Eu(im)(dpm)_3$ (im = imidazole) [10], $Nd(bipy)(dpm)_3$ (bipy = 2,2'-bipyridine) [11], $Gd(bipy)(dpm)_3$ [12], $Tb(bipy)(dpm)_3$, $Tb(phen)(dpm)_3$ [13], and $La(phen)(dpm)_3$ (phen = 1,10-phenanthroline) [14]. However, the functional properties of these ligands have never been studied.

In the present work we synthesized mixed-ligand europium(III) (**I**) and terbium(III) (**II**) dipivaloylmethanate complexes with such N-heterocyclic ligands as 3,5-dimethylpyrazole (dmpz), imidazole, 4-aminopyridine (apy), 2,2'-bipyridine, and 1,10-phenanthroline and studied their thermal and luminescent properties. The structure of certain complexes was established by X-ray diffraction analysis.

Mixed-ligand complexes **III–XII** were prepared by the reactions of compounds **I** and **II** and N-ligands in nonaqueous solvents (toluene, ethanol) [13]. Table 1 lists the elemental analyses and melting points of the resulting complexes.

According to X-ray diffraction (XRD) data, complexes **III–VIII** are polycrystals. The XRD patterns of the Eu(III) and Tb(III) complexes with the same N-ligands are similar to each other. The XRD patterns of all the mixed-ligand complexes show no peaks characteristic of the starting chelates **I** and **II** and nitrogenous heterocycles. Indexing was performed using the XRD patterns calculated using experimental XRD data. Most of the complexes studied are single-phase, except for complexes **IX** and **X**, whose XRD patterns contain, along with peaks of the main

Table 1. Elemental analyses and melting points of compounds **I–XII**

Comp. no.	mp, °C	Found, %			Formula	Calculated, %		
		C	H	N		C	H	N
I	192–193	56.4	8.2	–	$C_{33}H_{57}EuO_6$	56.5	8.2	–
II	182–183	55.8	8.2	–	$C_{33}H_{57}O_6Tb$	55.9	8.1	–
III	130–131	57.3	8.1	3.6	$C_{38}H_{65}EuN_2O_6$	57.2	8.2	3.5
IV	129–130	56.5	8.2	3.5	$C_{38}H_{65}N_2O_6Tb$	56.7	8.1	3.5
V	206–207	56.2	8.1	3.5	$C_{35}H_{61}EuN_2O_6$	56.2	8.0	3.6
VI	210–211	55.6	7.8	3.6	$C_{35}H_{61}N_2O_6Tb$	55.7	7.9	3.6
VII	174–175	57.2	8.2	3.5	$C_{38}H_{63}EuN_2O_6$	57.4	8.0	3.5
VIII	175–176	57.0	8.0	3.5	$C_{38}H_{63}N_2O_6Tb$	56.9	7.9	3.5
IX	195–196	60.1	7.5	3.4	$C_{38}H_{63}EuN_2O_6$	60.2	7.6	3.3
X	199–200	59.8	7.5	3.3	$C_{38}H_{63}N_2O_6Tb$	59.7	7.6	3.2
XI	237–238	61.2	7.3	3.4	$C_{38}H_{63}EuN_2O_6$	61.3	7.4	3.2
XII	254–255	60.6	7.2	3.4	$C_{38}H_{63}N_2O_6Tb$	60.8	7.4	3.2

component, a number of unidentified weak peaks. Probably, the samples of complexes **IX** and **X** contain an admixture of another crystal modification of these complexes.

The structure of the starting chelate **I** was studied by X-ray analysis (Table 2 and 3). The crystal of chelate I consists of discrete dimers $[Eu_2(dpm)_6]$ (Fig. 1). This complex is similar in structure to previously studied complexes $[Tb_2(dpm)_6]$ [13], $[Pr_2(dpm)_6]$ [15], and $[Gd_2(dpm)_6]$ [16]. Four ligands are coordinated of the Eu atoms in a bidentate cyclic mode, and the other two ligands are coordinated in a bidentate bridging mode. Each Eu atom coordinates

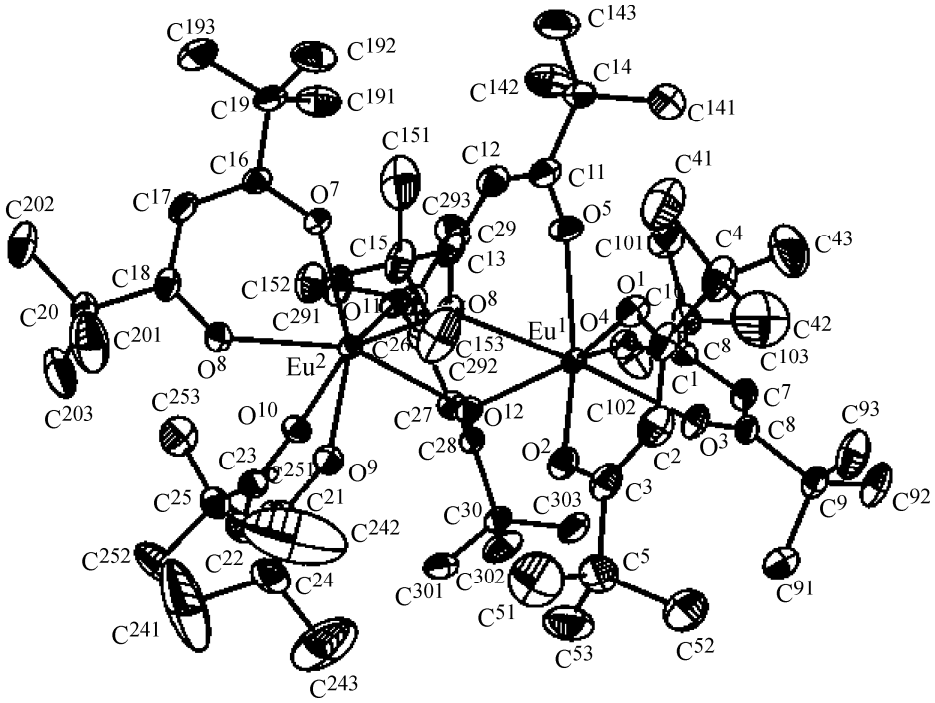

Fig. 1. General view of a molecule of chelate $[Eu_2(dpm)_6]$ (**I**) (H atoms are not shown).

Table 2. Crystal data and conditions of diffraction experiment for complexes **I–IV** and **VIII**

Parameter	**I**	**III**	**IV**	**VIII**
Formula	$C_{66}H_{114}Eu_2O_{12}$	$C_{38}H_{65}EuN_2O_6$	$C_{38}H_{65}N_2O_6Tb$	$C_{38}H_{63}N_2O_6Tb$
M	1403.49	797.89	804.85	802.82
Temperature, K	150(2)	150(2)	150(2)	150(2)
Syngony	Monoclinic	Triclinic	Triclinic	Monoclinic
Space group	$P2_1/n$	$P\bar{1}$	$P\bar{1}$	$P2_1/n$
a, *Å*	12.267(2)	9.7938(6)	9.794(1)	20.5754(12)
b, Å	27.763(4)	11.7413(7)	11.709(1)	10.1837(6)
c, Å	21.958(3)	19.1189(13)	19.163(2)	21.8932(13)
α, deg		75.231(2)	75.001(2)	
β, deg	105.170(4)	80.075(2)	80.168(2)	112.781(2)
γ, deg		81.601(2)	81.387(2)	
V, Å^3	7217.4(18)	2082.0(2)	2078.5(4)	4229.5(4)
Z	4	2	2	4
D_{calc}, g/cm^3	1.292	1.273	1.286	1.261
μ(MoK_a), mm^{-1}	1.775	1.548	1.743	1.713
F(000)	2928	836	840	1672
Crystal dimensions, mm	0.34×0.26×0.14	0.20×0.06×0.03	0.30×0.15×0.06	0.38×0.20×0.04
θ range, deg	1.21–32.16	1.80–30.71	1.81–31.75	1.73–31.17
Number of measured reflections	95344	21840	42125	101113
Number of unique reflections	25163 (R_{int} 0.0297)	12715 (R_{int} 0.0433)	14048 (R_{int} 0.0238)	13656 (R_{int} 0.0434)
Completeness to θ = 25.00, %	99.1	99.8	99.9	99.9
Transmission, min/max	0.584/0.789	0.895 / 0.955	0.738 / 0.901	13656 / 2 / 495
S-Factor on F^2	1.105	1.007	1.027	1.079
R-Factor on $I > 2\sigma(I)$	R_1 0.0361, wR_2 0.0786	R_1 0.0464, wR_2 0.0827	R_1 0.0242, wR_2 0.0556	R_1 0.0327, wR_2 0.0689
R-Factor on all reflections	R_1 0.0493, wR_2 0.0849	R_1 0.0768, wR_2 0.0936	R_1 0.0303, wR_2 0.0581	R_1 0.0460, wR_2 0.0721
min/max, *e*/A^3	–0.917/2.279	–1.130/1.456	–0.838/1.021	–0.860/1.503

seven O atoms to form a coordination polyhedron as a distorted one-cap trigonal prism. The dimeric structure consists of two such prisms sharing a face [$O^6\cdots O^{12}$].The Eu atoms are at a distance of 3.9807(4) Å from each other. The Eu bonds with bridging O atoms are longer that the Eu bonds with the O atoms of bidentate cyclic ligands [O–C 1.252(3)–1.321(3), C_{sp2}–C_{sp2} 1.384(4)–1.431(4), C_{sp2}–C_{sp3} 1.538(3)–1.554(4), C_{sp3}–C_{sp3} 1.476(6)–1.548(5) Å].

It should be noted that the O–C distance in bidentate bridging ligands [O^6–C^{13} 1.319(3) and O^{12}–C^{28} 1.321(3) Å] is slightly longer that in bidentate cyclic ligands [O–C 1.252(3)–1.281(3) Å]. The Eu coordina-

Table 3. Principal bond lengths (*d*, Å) and angles (ω, deg) in complexes **I, III, IV**, and **VIII**

I				III		IV		VIII	
bond, angle	*d*, ω	bond, angle	*d*, ω	bond, angle	*d*, ω	bond, angle	*d*, ω	bond, angle	*d*, ω
$Eu^1–O^4$	2.315(2)	$Eu^2–O^7$	2.302(2)	Eu–O^1	2.320(2)	Tb–O^1	2.300(1)	Tb–O^4	2.262(2)
$Eu^1–O^1$	2.316(2)	$Eu^2–O^{10}$	2.304(2)	Eu–O^2	2.340(2)	Tb–O^2	2.314(1)	Tb–O^1	2.284(2)
$Eu^1–O^2$	2.334 (2)	$Eu^2–O^9$	2.317(2)	Eu–O^3	2.340(2)	Tb–O^3	2.317(1)	Tb–O^3	2.309(2)
$Eu^1–O^3$	2.343 (2)	$Eu^2–O^{11}$	2.358(2)	Eu–O^4	2.367(2)	Tb–O^4	2.339(1)	Tb–O^6	2.314(2)
$Eu^1–O^5$	2.352(2)	$Eu^2–O^8$	2.360(2)	Eu–O^5	2.306(2)	Tb–O^5	2.278(1)	Tb–O^2	2.319(2)
$Eu^1–O^{12}$	2.415(2)	$Eu^2–O^6$	2.412(2)	Eu–O^6	2.312(3)	Tb–O^6	2.289(1)	Tb–O^5	2.323(2)
$Eu^1–O^6$	2.462(2)	$Eu^2–O^{12}$	2.462(2)	Eu–N^1	2.536(3)	Tb–N^1	2.510(1)	Tb–N^1	2.56(2)
$O^4Eu^1O^1$	123.46(7)	O^7EuO^{10}	122.65(7)	O^5EuO^6	73.37(8)	O^5TbO^6	74.17(4)	O^4TbO^1	126.95(6)
$O^4Eu^1O^2$	137.95(7)	$O^7Eu^2O^9$	138.58(7)	O^5EuO^1	85.20(9)	O^5TbO^1	84.73(5)	O^4TbO^3	74.47(6)
$O^1Eu^1O^2$	74.19(7)	$O^{10}Eu^2O^9$	74.08(7)	O^6EuO^1	80.84(9)	O^6TbO^1	80.45(5)	O^1TbO^3	138.81(6)
$O^4Eu^1O^3$	71.68(6)	$O^7Eu^2O^{11}$	77.31(6)	O^5EuO^3	81.57(8)	O^5TbO^2	132.20(4)	O^4TbO^6	78.24(6)
$O^1Eu^1O^3$	78.85(7)	$O^{10}Eu^2O^{11}$	79.87(7)	O^6EuO^3	143.77(8)	O^6TbO^2	137.44(4)	O^1TbO^6	78.67(6)
$O^2Eu^1O^3$	76.07(6)	$O^9Eu^2O^{11}$	143.58(7)	O^1EuO^3	123.19(9)	O^1TbO^2	71.70(4)	O^3TbO^6	142.39(6)
$O^4Eu^1O^5$	76.38(6)	$O^7Eu^2O^8$	71.28(7)	O^5EuO^2	132.43(8)	O^5TbO^3	81.24(4)	O^4TbO^2	80.21(6)
$O^1Eu^1O^5$	78.06(7)	$O^{10}Eu^2O^8$	77.63(7)	O^6EuO^2	137.51(8)	O^6TbO^3	144.23(4)	O^1TbO^2	72.71(6)
$O^2Eu^1O^5$	144.62(7)	$O^9Eu^2O^8$	77.25(7)	O^1EuO^2	70.83(8)	O^1TbO^3	123.10(5)	O^3TbO^2	78.52(6)
$O^3Eu^1O^5$	119.50(7)	$O^{11}Eu^2O^8$	121.51(7)	O^3EuO^2	78.66(8)	O^2TbO^3	78.25(4)	O^6TbO^2	121.67(6)
$O^4Eu^1O^{12}$	83.18(6)	$O^7Eu^2O^6$	84.95(6)	O^5EuO^4	86.31(8)	O^5TbO^4	86.34(5)	O^4TbO^5	88.45(6)
$O^1Eu^1O^{12}$	152.20(6)	$O^{10}Eu^2O^6$	151.96(6)	O^6EuO^4	80.51(9)	O^6TbO^4	79.98(5)	O^1TbO^5	127.64(6)
$O^2Eu^1O^{12}$	91.28(7)	$O^9Eu^2O^6$	88.39(7)	O^1EuO^4	161.05(9)	O^1TbO^4	160.07(5)	O^3TbO^5	81.60(6)
$O^3Eu^1O^{12}$	121.21(6)	$O^{11}Eu^2O^6$	104.09(7)	O^3EuO^4	72.03(8)	O^2TbO^4	126.60(4)	O^6TbO^5	72.20(6)

tion to ligands closes six-membered chelate ring EuO_2C_3. Two ligands [$O^1O^2C^1–C^3$ (*1*) and $O^3O^4C^6–C^8$ (*2*) in the Eu^1 molecule and $O^7O^8C^{16}–C^{18}$ (*4*) and $O^9O^{10}C^{21}–C^{23}$ (*5*) in the Eu^2 molecule] are almost planar (the deviations of atoms from the mean ring plane are not larger than 0.04 Å), and the third ligand [$O^5O^6C^{11}–C^{13}$ (*3*) in the Eu^1 molecule and $O^{11}O^{12}C^{26}–C^{28}$ (*6*) in the Eu^2 molecule] has a *sofa* conformation: the bending angles along the $O^{5\cdots6}$ and $O^{11\cdots}O^{12}$ lines are 39.5° and 42.7°, respectively. The interligand angles are 97.5° (1/2), 68.9° (1/3), 80.4° (2/3), 102.9° (4/5), 79.5° (4/6), and 68.7° (5/6).

According to X-ray diffraction data, complexes **III** and **IV** are isostructural. Their crystal structures consist of isolated $Ln(dmpz)(dpm)_3$ (Ln = Eu, Tb) molecules (Fig. 2). The metal atom is linked to six O atoms of three bidentate cyclic dipivaloylmethanate ligands and the dimethylpyrazole nitrogen atom (Table 3), thus forming a coordination polyhedron as a distorted one-cap trigonal prism. The bond lengths and bond angles in the three crystallographically independent dipivaloylmethanate ligands are close to each other [O–C 1.251(4)–1.286(4), $C_{sp2}–C_{sp2}$ 1.380(5)–1.407(5), $C_{sp2}–C_{sp3}$ 1.530(5)–1.547(4), and $C_{sp3}–C_{sp3}$ 1.488(7)–1.544(5) Å in complex **III**; O–C 1.257(2)–1.285(2), $C_{sp2}–C_{sp2}$ 1.388(2)–1.410(2), $C_{sp2}–C_{sp3}$ 1.537(2)–1.542(2), $C_{sp3}–C_{sp3}$ 1.485(4)–1.541(3) Å in complex **IV**].

The coordination of the metal atom to dipivaloylmethanate ligands closes six-membered chelate

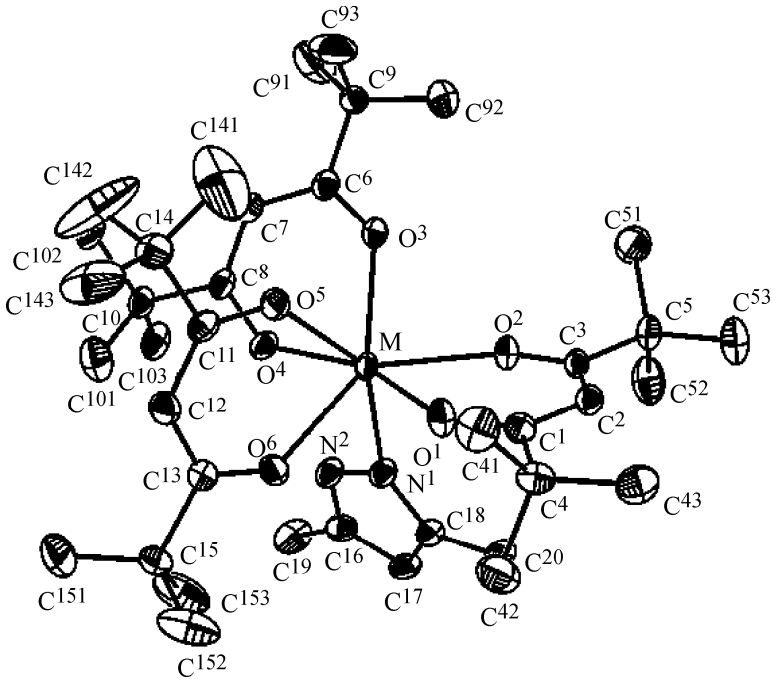

Fig. 2. General view of molecules of complexes Ln(dmpz)(dpm)$_3$ (**III, IV**) [Ln = Eu(III), Tb(III)] (H atoms are not shown).

rings LnO_2C_3. Two ligands [$O^1O^2C^1$–C^3 (*1*) and $O^5O^6C^{11}$–C^{13} (*2*)] in complexes **III** and **IV** are almost planar (the deviations of atoms from the mean ring plane are not larger than 0.02 Å); the third ligand [$O^3O^4C^6$–C^8 (*3*)] has a *sofa* conformation: the Ln atom deviates from the ligand plane by 0.74 Å, and the bending angle along the $O^3\cdots O^4$ line is 157.0° in both complexes. The angles between the six-membered ring planes are 88.4° and 89.0° (1/2), 114.4° and 114.4° (1/3), and 123.0° and 121.8° (2/3) in complexes **III** and **IV**, respectively. The dimethylpyrazole molecules in structures **III** and **IV** are almost planar, and the deviations of atoms from the ring planes were no larger than 0.01 Å.

The crystal structure of complex **VIII** consists of isolated Tb(apy)(dpm)$_3$ molecules (Fig. 3). The Tb atom is linked to six O atoms of three bidentate cyclic dipivaloylmethanate ligands and the 4-aminopyridine nitrogen atom (Table 3) to form a distorted one-cap trigonal prism. The bond lengths and bond angles in the three crystallographically independent dipivaloylmethanate ligands are close to each other [O–C 1.260(3)–1.276(3), C_{sp2}–C_{sp2} 1.390(3)–1.407(3), C_{sp2}–C_{sp3} 1.537(3)–1.542(3), C_{sp3}–C_{sp3} 1.455(5)–1.563(6) Å]. The coordination of the metal atom to dipivaloylmethanate ligands closes six-membered chelate rings TbO_2C_3. Two ligands [$O^1O^2C^1$–C^3 (*1*) and $O^3O^4C^6$–C^8 (*2*)] are almost planar (the deviations of atoms from the mean ring plane are not larger than 0.02 Å). The third ligand [$O^5O^6C^{11}$–C^{13} (*3*)] has a *sofa* conformation: the Tb atom deviates from the plane of the dipivaloylmethanate ligand by 0.2467 Å, and the bending angle along the $O^5\cdots O^6$ line is 28.9°. Furthermore, disorder of carbon atoms in one of the *t*-Bu groups in this ligand is observed. The angles between the six-membered ring planes are 77.3 (1/2), 74.8 (1/3), and 104.8° (2/3).

4-Aminopyridine atoms in the structure of complex **VIII** are disordered. The N–C and C–C bond lengths in the almost planar ligand molecules are 1.28(2)–1.37(2) and 1.36(1)–1.42(2) Å, respectively (the deviations of atoms from the mean planes of the rings are no larger than 0.01 Å). The bond lengths in the 4-aminopyridine molecule agree well with published data [17]. The dihedral angles between the dipivaloylmethanate and 4-aminopyridine planes are 59.4°, 40.9°, and 125.6°. There are N–H···O contacts ($O^6\cdots H^{2'}$ 2.341, $O^6\cdots N^{2'}$ 3.087 Å) between noncoordinated amino groups and the dipivaloylmethanate ligands.

The fact that the experimental XRD patterns of complexes **III, IV**, and **VIII** are coicident with those calculated from the XRD analysis data suggests structural similarity of the synthesis products and single crystals. These findings provide evidence for

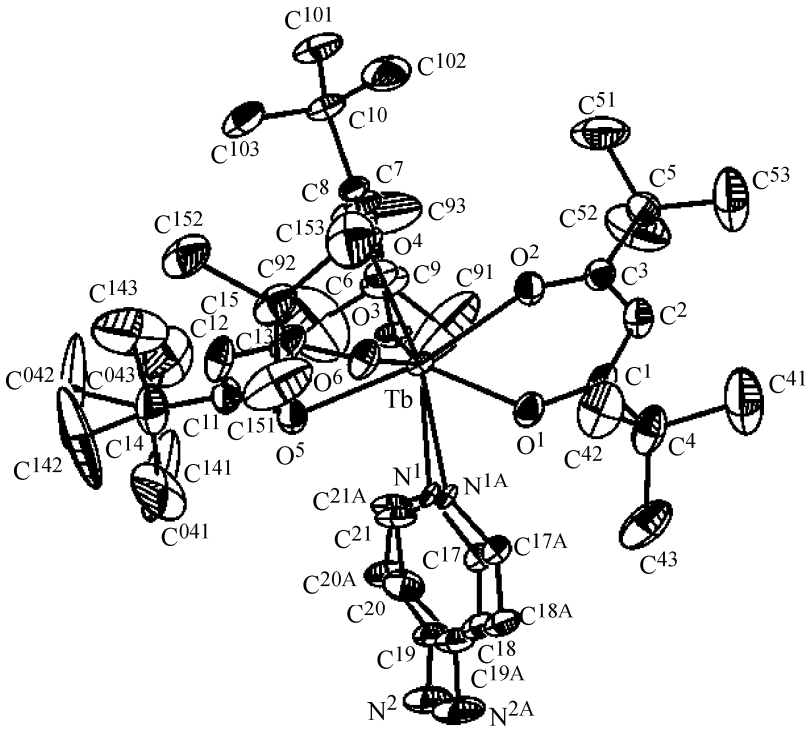

Fig. 3. General view of a molecule of complex Tb(apy)(dpm)$_3$ (**VIII**) (H atoms are not shown).

our conclusion that the synthesized mixed-ligand complexes for the most part are single-phase.

Thermogravimetric analysis of chelates **I** and **II** and mixed-ligand complexes **III–XII** under heating to 350°C in an inert atmosphere gave almost complete evaporation. Terbium(III) compounds showed a slightly higher volatility compared to Eu(III) compounds. This is probably explained by the fact that Tb(III) complexes are less associated due to a smaller ionic radius of the Tb(III) atom and its better shielding by the ligands. Imidazole (Fig. 4a), 4-dimethylpyrazole, 4-aminopyridine, and 2,2'-bipyridine evaporate at temperatures lower by 50–80°C than chelates **I** and **II**. At the same time, the weight loss curves of mixed-ligand complexes containing these compounds are only slightly shifted to the high-temperature region compared to the TG curves of chelates **I** and **II**. Consequently, the coordination of N-heterocyclic ligands to chelates **I, II** to form mixed-ligand complexes did not affect the thermal properties of the starting chelates. Unlike the other N-heterocycles, phenanthroline evaporates at temperatures higher by 30–40°C than chelates **I** and **II**. Mixed-ligand complexes **XI** and **XII**, too, evaporated at higher temperatures (Fig. 4b). Consequently, the coordination of phenanthroline to chelates **I** and **II** to form Ln(phen)(dpm)$_3$ reduces the volatility of the starting chelates. Thus, most of the mixed-ligands chelates are as volatile as chelates **I** and **II**, except for Ln(phen)(dpm)$_3$. These results showed that mixed-ligand complexes **III–XII** can be used to prepare their films by chemical vapor deposition.

The luminescence data for the synthesized compounds are given in Table 4. Unlike chelate **I**, chelate **II** exhibits a bright photoluminescence. The photoluminescence spectrum of this compound has four bands at λ_{max} 490, 545, 585, and 620 nm associated with the $^5D_4 \rightarrow {}^7F_6$, $^5D_4 \rightarrow {}^7F_5$, $^5D_4 \rightarrow {}^7F_4$, and $^5D_4 \rightarrow {}^7F_3$ transitions, respectively. The "green" line at λ_{max} 545 nm has the highest intensity. The photoluminescence spectrum of the solid phase obtained by evaporation of the toluene solution of an equimolar mixture of the isostructural chelates **I** and **II** contains, along with the photoluminescence bands of the Tb^{3+} ion, a weak band at 615 nm, corresponding to the $^5D_0 \rightarrow {}^7F_2$ transition in the Eu^{3+} ion. Apparently, the evaporation of the solution of complexes **I** and **II** forms a solid solution, which makes possible $Tb^{3+} \rightarrow Eu^{3+}$ energy transfer with subsequent development of Eu^{3+} photoluminescence. The photoluminescence spectrum of a mechanical mixture of solid chelates **I** and **II** have no other bands than those of chelate **II**.

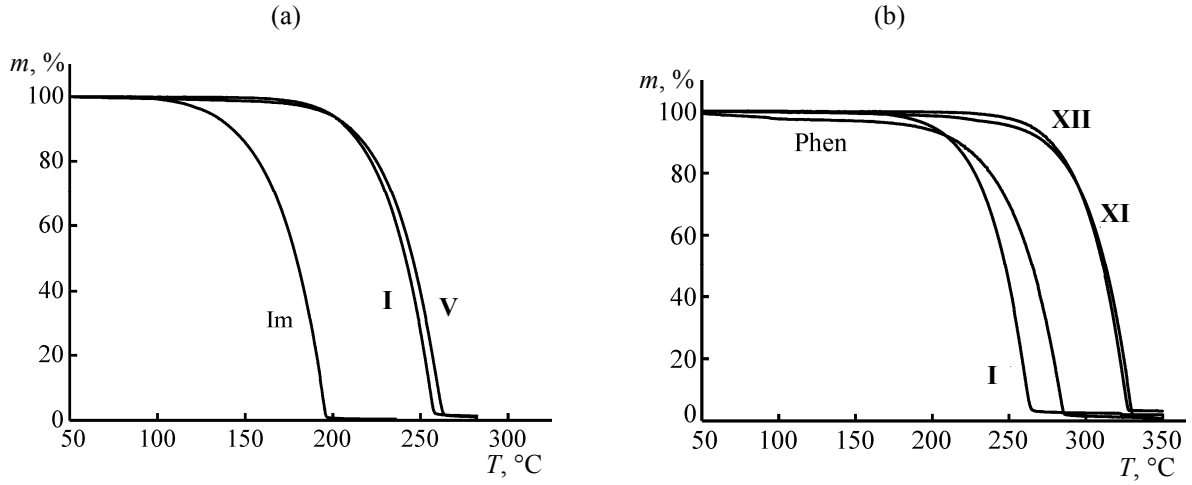

Fig. 4. TG curves of (a) compounds **I** and **V** and imidazole and (b) complexes **I, XI**, and **XII** and 1,10-phenanthroline.

We also studied the luminescence of the solid phases of the Eu(phen)$(dpm)_3$–Tb(phen)$(dpm)_3$ system, obtained by evaporation of toluene solutions of mixtures of the complexes with varied component ratio. For comparisons we chose the intensity of the strongest photoluminescence band of Eu(III) compounds at 615 nm. Terbium(III) complexes show no photoluminescence at this wave length. The measurement results are presented in Fig. 5.

As seen, at voltages of 600 and 700 V and complex **XII** concentrations of 25–5%, the photoluminescence of the system is stronger compared to the individual complex **XI**. This suggests $Tb^{3+} \rightarrow Eu^{3+}$ energy transfer. The strongest luminescence is characteristic of the solid phase comprising 90% of complex **XI** and 10% of complex **XII**. However, this effect is not observed at 500 V.

The high volatility of the studied compounds allows preparation of their films, which was demonstrated by the examples of complexes **II** and **IV**. According to XDR data, the resulting films are amorphous. Comparison of the IR spectra of the films and finely dispersed compounds **II** and **VI** showed that these compounds undergo no thermolysis during chemical

Table 4. Photoluminescence intensities (rel. units) of compounds **I–XII**

Comp. no.	$^5D_4 \rightarrow {}^7F_6$ (490 nm)	$^5D_4 \rightarrow {}^7F_5$ (545 nm)	$^5D_4 \rightarrow {}^7F_4$ (585 nm)	$^5D_4 \rightarrow {}^7F_3$ (620 nm)	$^5D_0 \rightarrow {}^7F_1$ (595 nm)	$^5D_0 \rightarrow {}^7F_2$ (615 nm)
I	–	–	–	–	–	2
II	140	630	25	15	–	–
III	–	–	–	–	–	5
IV	225	740	30	20	–	–
V	–	–	–	–	–	5
VI	205	695	30	15	–	–
VII	–	–	–	–	–	5
VIII	230	720	30	20	–	–
IX	–	–	–	–	15	20
X	110	220	20	5	–	–
XI	–	–	–	–	5	75
XII	5	15	–	–	–	–

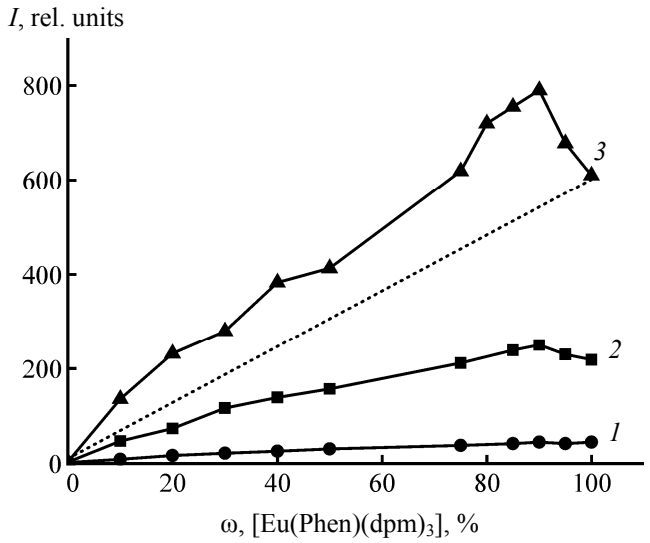

Fig. 5. Dependence of the luminescence intensity at 615 nm of the $Tb(phen)(dpm)_3$–$Eu(phen)(dpm)_3$ solutions on their composition. Voltage, V: (*1*) 500, (*2*) 600, and (*3*) 700 (λ_{ex} 330 nm).

vapor deposition. According to electron microscopy data, the films have a granular structure with a 1-μm grain size. These films, too, showed photoluminescence, and, therewith, the bands in their spectra and in the photoluminescence spectra of solid complexes **II** and **VI** are in the same positions. The photoluminescence intensity of the films did not change for a long time, providing evidence for their stability and potential use as promising luminescent materials.

EXPERIMENTAL

In the work we used $EuCl_3 \cdot 6H_2O$ and $TbCl_3 \cdot 6H_2O$ (pure), dipivaloylmethane (Dalchem), NaOH (analytical grade), N-heterocyclic compounds (chemical and analytical grades), ethanol (rectificate); and heptane, benzene, and toluene (analytical grade).

Elemental analysis was performed on a EuroEA 3000 analyzer. The melting points were determined on a Boëtius hot stage. The IR spectra were measured on a Scimitar FTS 2000 spectrometer in KBr in the range 375–4000 cm^{-1}. Thermogravimetry was performed using a NETZSCH TG 209 F1 Iris thermomicrobalance (sample weight ~7 mg, aluminum crucible) in a helium atmosphere, gas flow rate 60 mL/min, heating rate 10 deg/min. The results were treated using Proteus Analysis software [19].

The photoluminescence spectra were measured on a Cary Eclipse Varian spectrophotometer at 300 K (*U* 500, 600, and 700 V, slit 5 nm).

The XRD analysis was performed at 300 K on a Shimadzu XRD-7000 diffractometer (CuK_α radiation, Ni filter, 2θ 5°–60°). Samples were ground in an agate mortar and then applied on a polished side of a standard quartz cell, coated with a thin layer of mineral oil. The external reference was a polycrystalline silicon sample prepared in a similar way.

Chelates **I** and **II** were synthesized as described in [4, 13, 18]. The resulting powdered chelates **I** and **II** were purified by double sublimation in a vacuum gradient (250°C, 1×10^{-2} Torr). The yields were ~80% (per $LnCl_3$).

Synthesis of complexes III–XII. A mixture of 0.1 mmol (~0.07 g) of Ln(III) dipivaloylmethanate and 0.1 mmol of N-heterocyclic ligand was dissolved with heating in toluene or alcohol [13]. The solvent was evaporated to form finely dispersed reaction products in near-quantitative yields.

X-ray diffraction analysis. Single crystals of chelate **I**, suitable for analysis, were grown from benzene solutions under cooling. Single crystals of mixed-ligand complexes **III, IV**, and **VIII** were obtained by evaporation of their toluene solutions. The unit cell parameters and intensity data were collected at 150(2) K on a Bruker Apex DUO automated diffractometer with a CCD detector by a standard procedure (MoK_α radiation, graphite monochromator). The crystal data and experimental details are presented in Table 2, and the principal bond length and angles are listed in Table 3. Absorption was included semiempirically using SADABS software [20]. The structures were solved by the direct method and refined by full-matrix least squares on F^2 anisotropically for non-hydrogen atoms using SHELX97 software [21]. Hydrogen atoms were located geometrically and refined in a rigid body approximation. The crystal data for complexes **I, III, IV**, and **VIII** were deposited in a Cambrige structural database (CCDC 1007504–1007507).

ACKNOWLEDGMENTS

The work was financially supported by the Russian Foundation for Basic Research (project no. 14-03-00386a) and Ministry of Education and Science of the Russian Federation.

REFERENCES

1. Katkova, M.A., Bochkarev, M.N., and Vitukhnovsky, A.G., *Russ. Chem. Rev*., 2005, vol. 74, no. 12, p. 1089. DOI: 10.1070/RC2005v074n12ABEH002481.
2. Katkova, M.A. and Bochkarev, M.N., *Dalton Trans.,* 2010, vol. 39, p. 6599. DOI:10.1039/C001152E.
3. Bochkarev, M.N., Vitukhnovskii, A.G., and Katkova, M.A., *Organicheskie svetoizluchayushchie diody* (Organic Light-Emitting Diodes), Nizhny Novgorod: Dekom, 2011.
4. Belaya, S.V., Bakovets ,V.V., Lobzareva, M.N., Boronin, A.I., Koshcheev, S.V., Korol'kov, I.V., and Stabnikov, P.A., *Neorg. Mater*., 2014, vol. 50, no. 4, p. 410.
5. Zou Gang, Zhang Yanze, and He Pingsheng, *Thin Solid Films*, 2004, vol. 468, p. 268. DOI: 10.1016/j.tsf.2004.06.114.
6. *Problemy khimii i primeneniya β-diketonatov metallov* (Problems of Chemistry and Application of Metal β-Diketonates), Spitsyn, V.I., Es., Moscow: Nauka, 1982, p. 100.
7. Cramer, R.E. and Seff, K., *Acta Crystallogr., Sect. B*, 1972, vol. 28, p. 3281. DOI: 10.1107/S056774087200785X.
8. Wasson, S.J.S., Sands, D.E., and Wagner, W.F., *Inorg. Chem.,* 1973, vol. 12, no. 1, p. 187. DOI: 10.1021/ic50119a042.
9. Clegg, W., Sage, I., Oswald, I., Brough, P., and Bourhill, G., *Acta Crystallogr., Sect. C*, 2000, vol. 56, p. 1323. DOI: 10.1107/S0108270100011641.
10. Wayda, A.L., Kaplan, M.L., Lyons, A.M., and Rogers, R.D., *Polyhedron*, 1990, vol. 9, p. 751. DOI: 10.1016/S0277-5387(00)80285-5.
11. Korytnyy, E.F., Dzyubenko, N.G., Aslanov, A.A., and Martynenko, L.I*., Zh. Neorg. Khim*., 1981, vol. 26, no. 1, p. 72.
12. Minacheva, L.Kh., Rogachev, A.Yu., Sergienko, V.S., and Kuz'mina, N.P., *Russ. J. Coord. Chem*., 2005, vol. 31, no. 10, p. 725. DOI: 10.1007/s11173-005-0160-9.
13. Stabnikov, P.A., Zharkova, G.I., Smolentsev, A.I., Pervukhina, N.V., and Krisyuk, V.V., *J. Struct. Chem*., 2011, vol. 52, no. 3, p. 560. DOI: 10.1134/S0022476611030176.
14. Minacheva, L.Kh., Rogachev, A.Yu., Kuz'mina, N.P., and Sergienko, V.S., *Russ. J. Inorg. Chem*., 2003, vol. 48, p. 2.
15. Mode, V.A. and Smith, G.S., *J. Inorg. Nucl. Chem*., 1969, vol. 31, no. 6, p. 1857. DOI: 10.1016/0022-1902(69)80407-0.
16. Baxter, I., Drake, S.R., Hursthouse, M.B., Abdul Malik, K.M., McAleese, J., Otway, D.J., and Plakatouras, J.C., *Inorg. Chem*., 1995, vol. 34, no. 6, p. 1384. DOI: 10.1021/ic00110a016.
17. Allen, F.H., Kennard, O., and Watson, D.G., *J. Chem. Soc. Perkin Trans.*, 1987, vol. 1, S1. DOI: 10.1039/P298700000S1.
18. Eisentraut, K.J. and Sievers, R.E*., J. Am. Chem. Soc*., 1965, vol. 87, no. 22, p. 5254. DOI:10.1021/ja00950a051.
19. *NETZSCH Proteus Thermal Analysis*, Version 4.8.1, Bayern: NETZSCH-Geratebau, 2005.
20. *Bruker AXS APEX2* (Version 1.08), SAINT (Version 7.03), and *SADABS* (Version 2.11), Madison, WI: Bruker Ådvanced X-ray Solutions, 2004.
21. Sheldrick, G.M., *SHELX97*, Release 97-2, Göttingen: Univ. Göttingen, 1998.